Validation of Early Synapse Loss

in a Mouse Model of Frontotemporal Dementia

by

Hannah Weisman

A Thesis Presented in Partial Fulfillment
of the Requirements for the Degree
Master of Science

Approved May 2022 by the
Graduate Supervisory Committee:

Rita Sattler, Chair
Diego Mastroeni
Ramón Velázquez

ARIZONA STATE UNIVERSITY

August 2022

ABSTRACT

Frontotemporal dementia (FTD) is a neurodegenerative disease that causes deterioration of the frontal and temporal lobe. Detection is pivotal in preventative care, but current screening methods are not sensitive enough to detect early-stage disease. Synapse loss has been implicated as an early contributor to neurodegeneration and subsequent atrophy. Fluorine-18 fluorodeoxy-glucose (18[F]-FDG) positron emission tomography (PET) is a noninvasive imaging biomarker method frequently used as a surrogate measure for synaptic activity in the brain. PET scans using 18[F]-FDG tracers were performed on progranulin (GRN) knockout mice ($Grn^{-/-}$), a commonly used mouse model of FTD. Interestingly, 18[F]-FDG PET at both, 9 months and 11 months, two time points considered early symptomatic in the $Grn^{-/-}$ mouse model, did not detect significant changes in synaptic activity, suggesting that no synapse loss has occurred yet at these early stages of FTD in this model. After the last PET scan, the imaging data were validated via fluorescent immunostaining for pre- and post-synaptic marker proteins SV2 and PSD95, respectively. Quantifications in several brain regions, including the frontal cortex, did not reveal any significant differences in protein expression, supporting the lack of aberrant 18[F]-FDG tracer uptake measured via PET. Additional examinations for activated microglia, a known aspect of FTD pathology recently observed in end $Grn^{-/-}$ mice, did not reveal microglia activation as measured via CD68 immunostaining. These data suggest that $Grn^{-/-}$ mice at 9 and 11 months do not exhibit synaptic dysfunction in

the frontal cortex when measured via 18[F]-FDG PET or immunostaining of pre- and postsynaptic marker proteins SV2 and PSD95.

ACKNOWLEDGMENTS

I am grateful for the many people who have helped me in my graduate school journey. First, I would like to acknowledge the work of my mentor Dr. Rita Sattler who encouraged me to challenge myself to think bigger. Rita brought me into her lab despite the difficult timing and I will always be grateful for the patience she showed me. Next, I would like to thank Dr. Ileana Lorenzini for her support in the lab. She has always been available for questions, advice and just chatting in general. The work by Jennifer Levy, Mo Singer, Lynette Bustos, Ryan Pevey, Lauren Gittings, Stephen Moore and Camelia Burciu who were always available to remind me that none of the hurdles I faced couldn't be handled. Thank you to the professors that fostered my interest in neuroscience and genetics. Dr. Kenneth Buetow, Dr. Sam McClure and Dr. Marco Mangone all showed me the fascinating aspects of science that inspired me to want to learn more. I would also like to extend my gratitude to the Quarles Lab for their collaborative efforts in collecting the PET imaging data.

Thank you to the faculty and administration at Barrow Neurological Institute for maintaining an environment that allowed the work described here to be performed. Thank you to all of those at Arizona State University for their assistance throughout the graduate program.

TABLE OF CONTENTS

Page

LIST OF FIGURES iv

CHAPTER

1 INTRODUCTION ……..... 1

2 FRONTOTEMPORAL DEMENTIA ……..……..... 2

2.1 Clinical Spectrum of Frontotemporal Dementia..... 2

2.2 Genetics..... 3

2.3 Pathology..... 4

2.4. Proposed Mechanisms of Disease..... 5

2.4.1. Proteinopathies of TDP-43 and Tau..... 5

2.4.2 Synapse Loss 6

2.4.3 Microglia Activation and Inflammation..... 8

2.5 Familial FTD Due to Mutations in GRN..... 9

2.5.1 Loss of Function 9

2.5.2 Models of FTD GRN..... 10

2.5.3 Biomarkers for FTD GRN 11

3 HYPOTHESIS AND SPECIFIC AIMS……..... 14

4 METHODS 15

4.1 Breeding..... 15

4.2 PET Imaging..... 15

4.2.1 Acquisition 15

4.2.2 Analysis..... 16

CHAPTER Page

4.3 Perfusion..... 17

4.4 Immunohistochemistry..... 19

4.4.1 Imaging of Immunohistochemistry..... 19

4.4.2 Statistical Analysis……..... 19

5 RESULTS……..... 21

5.1 FDG PET Analysis..... 21

5.2 Frontal Cortex Synaptic Imaging and Analysis 23

5.3 Hippocampus Synaptic Imaging and Analysis 24

5.4 VPL Synaptic Imaging and Analysis..... 27

5.5 Frontal Cortex Glial Activity Imaging/Analysis..... 29

6 DISCUSSION 31

7 CONCLUSION……..... 35

REFERENCES……..... 36

LIST OF FIGURES

Figure Page

1. 18[F]-FDG PET of $Grn^{-/-}$ Mice ……....22

2. Frontal Cortex of 11 Months Old $Grn^{-/-}$ Mice Does Not Reveal Significant Changes in Synaptic Marker Proteins……..……....23

3. Hippocampus of 11 Months Old $Grn^{-/-}$ Mice Does Not Reveal Significant Changes in Synaptic Marker Proteins……..……26

4. Ventroposterolateral Thalamus of 11 Months Old $Grn^{-/-}$ Mice Does Not Reveal Significant Changes in Synaptic Marker Proteins……..……28

5. Frontal Cortex of 11 Months Old $Grn^{-/-}$ Mice Does Not Reveal Significant Activation of Microglia……..……...……30

CHAPTER 1

INTRODUCTION

Neurodegenerative diseases can rob patients of their ability to move, think and take care of themselves. The degradation of the frontal lobe can damage a patient's memory and emotional regulation through loss of executive function. Detection and diagnosis are pivotal in preventative care, but current screening methods are not sensitive enough to detect early-stage disease. Practitioners could drastically improve treatment and patient care through more advanced screening methods. Therefore, scientists have been exploring biomarkers to assess disease diagnosis as well as progression.

CHAPTER 2

FRONTOTEMPORAL DEMENTIA

2.1 Clinical Spectrum of Frontotemporal Dementia

Frontotemporal dementia (FTD) is a heterogeneous disease that causes degeneration of the frontal and temporal lobe. Patients with FTD will first exhibit signs of the disease through abnormal behaviors and sporadic emotional outbursts. These issues with social conduct can include impulsive behavior through sudden purchases or commitments, difficulty regulating emotions and issues with short term memory (Snowden et al., British Journal of Psychology, 2002). While these traits are often generally associated with advanced age, they can be significant indicators of neurological impairment. FTD accounts for approximately 20% of all dementia cases (Snowden et al., British Journal of Psychology, 2002). The clinical spectrum of FTD includes the following subtypes: the behavioral variant of FTD, language variants, semantic dementia and progressive non-fluent aphasia (Kertesz et al., 2005, Brain). There is a notable overlap of symptoms among other neurodegenerative diseases such as parkinsonian syndromes, progressive supranuclear palsy and corticobasal syndrome (Galimberti et al., 2015, Biological Psychiatry). The causes of FTD are becoming clearer as researchers explore genetic influences along with comorbidities with lifestyle and behavior. Confirmed risk factors include advanced age, male sex and familial history (Armon et al., 2003, Neuroepidemiology). Lifestyle behaviors such as drinking, smoking and high saturated fat diets are

associated with increased risk as well (Lian et al., 2019, Journal of Clinical Neuroscience).

2.2. Genetics

FTD is 30% familial and 70% sporadic, suggesting a degree of hereditary influence (Synofzik et al., 2012, Neurobiol. Aging). Three major genes dominate the familial forms of FTD: granulin precursor (GRN), microtubule associated protein tau (MAPT) and chromosome 9 open reading frame 72 (C9orf72).

GRN functions as a precursor to the protein progranulin. Loss of function mutations due to haploinsufficiency of the granulin gene are considered a major cause of FTD (Lee et al., 2013, Human Molecular Genetics). The impact of granulin on the nervous system is further reflected in the comorbidity of granulin mutations and neuronal ceroid lipofuscinosis (Smith et al., 2012, J. Hum. Genet). Granulin has a protective role in relation to the immune system. MAPT is a gene that encodes for the protein tau which helps to stabilize neurons in the brain. Tau is found within the neurons of the central nervous system and is involved in the polymerization and stabilization of microtubules (Galimberti et al., 2015, Biological Psychiatry). MAPT haplotype is an important genetic risk factor in multiple different tau proteinopathies (Chornenkyy et al., 2019, Lab Invest). Abnormal tau is often aggregated in several subtypes of FTD (Stanford et al., 2003, Brain).

The gene C9orf72 is not only associated with FTD but also amyotrophic lateral sclerosis (ALS). It is regarded for its hexanucleotide repeat that is found to be exponentially replicated in patients (Zu et al., 2013, Research Profiles). The

excess replication leads to overproduction of antisense and sense RNA, causing the subsequent translation of 5 different repeat associated non-ATG (RAN) proteins [poly(GP), poly(GR), poly(GA), poly(PR), poly(GP)] which accumulate and cluster in affected brain regions (Cook et al., 2020). C9orf72 is cited as a contributing factor to about 40% of familial FTD cases and 8% of sporadic cases (Chia et al., 2018, The Lancet Neurology).

2.3 Pathology

Confirmation of a clinical diagnosis of FTD, referred to as frontotemporal lobar degeneration (FTLD), often requires a pathological analysis of the patient's brain postmortem. FTD pathologically is characterized and subgrouped by protein aggregations such as Tar DNA binding protein 43 (TDP-43) and Tau (Neumann and Mackenzie, 2019, Neuropathol Appl Neurobiol). There is notable heterogeneity within each pathological subgroup that correlate with clinical subgroups. For FTD, 45% of patients show protein aggregation of the RNA binding protein TDP-43 and 45% of patients exhibit abnormal protein inclusions of tau. The remaining patients' pathology is described as either FTLD-FET and FTLD-UPS, which is characterized by protein aggregations of fused in sarcoma (FUS), Ewing's sarcoma (EWS) and TATA-binding protein associated factor 2N (TAF-15) or ubiquitin positive inclusions with unknown protein identity, respectively. This simplified division into 4 pathological FTLD groups can be further divided into subtypes within each of the 4 categories depending on the

shape of the protein inclusions and/or the cellular or anatomical location (Neumann and MacKenzie 2019, Neuropathol Appl Neurobiol).

2.4 Proposed mechanisms of disease

2.4.1. Proteinopathies of TDP-43 and Tau

Mutations of modulatory genes in reactive pathways can lead to misfolded proteins that, in the case of many neurodegenerative diseases, significantly contribute to cell death. As noted above, ~45% of FTD patients exhibit TDP-43 proteinopathy, which is characterized by cytoplasmic inclusions of TDP-43 (Niccoli et al., 2017, Human molecular genetics). TDP-43 is an essential RNA binding protein (RBP) involved in many steps of RNA metabolism, including transcription, splicing, maturation, stability, transport, translation, as well as micro and long non-coding RNA processing (Banks et al., 2008, Genome). Containing both a nuclear localization signal (NLS) and a nuclear export signal (NES), TDP-43 plays roles in both the nucleus and the cytoplasm and its trafficking is essential for its proper function (Constantinescu et al., 2019, Mol Imaging Biol) (Landau et al., 2011, Neuronol Aging). The cytoplasmic accumulation and nuclear depletion of TDP-43 has been well established as a pathological hallmark of neurodegenerative diseases including Alzheimer's disease (AD), Parkinson's disease and other AD related dementias. These cytoplasmic TDP-43 inclusions have been hypothesized to contribute to disease pathogenesis through either nuclear depletion of TDP-43, leading to the loss of its RNA

metabolic functions, and/or cytoplasmic inclusions leading to a toxic gain of function (Gendron et al., 2013, Alzheimer's Dis; Josephs and Nelson, 2015, Lab Invest). About 45% of FTD patients exhibit pathology of aggregated tau in its wild type form, without any genetic mutations. In addition, about 6.3% of familial FTD patients and 1.5% of sporadic FTD patients have mutations in the MAPT gene (Deleon and Miller, 2018, Handbook of Clinical Neurology). Tau protein aids in microtubule stabilization and assembly and mutations in MAPT can affect numerous cellular functions, including aggregation of tau in the cytoplasm (also known as neurofibrillary tangles), aberrant phosphorylation of tau and aberrant alternative splicing of tau at the C-terminus (Arai et al., 2009, Acta Neuropathol). Certain epitopes with high phosphorylation activity target sites such as Ser422 and Ser396/S404 and are associated with more advanced stages of pathology (Bi et al., 2011, PLoS ONE). Physiological alternative splicing of MATPS generates six protein isoforms of tau: 0N3R, 0N4R, 1N3R, 1N4R, 2N3R and 2N4R. In the adult nervous system, the 3R and 4R isoforms are present in equal amounts (Goedert et al., 1989, EMBO J). Several mutations in MAPT lead to a disrupted 3R/4R ratio which is thought to contribute to the above-mentioned dysfunctions of the tau protein in disease. How exactly aberrant tau splicing contributes to disease pathogenesis in FTD is still poorly understood.

2.4.2 Synapse Loss

There is growing evidence that FTD, but also ALS, are "synaptopathies", i.e., diseases that involve an early and progressive loss of glutamatergic

synapses that drives symptom progression (Tantaway et al., 2012, BMC Nephrol; Maiti et al., 2015, Neurosci Res). Synapses lost in these conditions are predominantly those landing on dendritic spines, the small (~1μm) actin-rich protrusions of dendritic membrane that comprise the postsynaptic element at over 90% of glutamatergic contacts. In Alzheimer's disease, axospinous synapse loss is the major driver of cognitive decline (Liu et al., 1999, Dement Geriatr Cogn Disord). This relationship holds for most or all other neurodegenerative conditions with a cognitive component (Bodea et al., 2016, J Neurochem), such as Parkinson's dementia (Clare et al., 2010, J Neurosci Res), schizophrenia (Landau et al., 2011, Neurobiol Aging), traumatic brain injury (TBI) (Colom-Cadena et al., 2020, Alzheimers Res Ther), the tauopathies (Spires-Jones and Hyman, 2014, Neuron) and many others– and stems from the fact that loss of connectivity is a loss of information and loci of plastic changes involved in memory formation. Emerging data suggest synapse loss also drives symptoms in FTD and ALS. Postmortem studies of FTD brains show large decreases in synapses in frontal and temporal lobes as well as striatum (Henstridge et al., 2017, Acta Neuropathol). Notably, synapse loss in ALS extends to the medial prefrontal cortex (mPFC), where it is greater in those with cognitive impairment (Ringholz et al., 2005, Neurology) consistent with the spread of pathology to frontal circuits affected in FTD.

Work in animal models has extended these findings to show that large reductions in glutamatergic synapses – particularly those with mature, mushroom shaped spines – are an early event in FTD, occurring before neuronal death or

dendritic atrophy. In mice modeling the effects of the shared FTD/ALS genes GRN (Lui et al., 2016, Cell), FUS (Birsa et al., 2020, Semin Cell Dev Biol), TDP-43 (Kwong et al., 2007, Acta Neuropathol) and UBQLN2 (Neumann et al., 2006, Science) on FTD-like phenotypes, synapse loss (especially mushroom spines) was observed in entorhinal, hippocampal (Henstridge et al., 2017, Acta Neuropathol) and frontal cortical areas (DeKosky and Scheff, 1990, Ann Neurol). Similar effects were seen in mice with “pure” FTD-causing MAPT mutations (Majoor-Krakauer et al., 1994, Neurology).

2.4.3 Microglia activation and Inflammation

Microglia are macrophages within the neuroimmune system that regulate the state of the central nervous system by both protecting and removing cells. To counteract harmful pathogens, they can secrete proinflammatory cytokines to protect or destroy neurons (Azam et al., 2021, Cells). When microglia experience loss of function, they could leave the harmful pathogens unchecked. If there is gain of function, there could be an excess of activity to the point where the microglia are removing beneficial cells (Ranshoff and Perry, 2009, Annu. Rev. Immunol). Changes in microglial behavior are noted as part of physiological neurodegenerative diseases such as Alzheimer's disease, Huntington’s disease and Parkinson’s disease (Azam et al., 2021, Cells). The compromised microglia then damage the environment by increasing defensive functions that cause neuroinflammation and cell death.

2.5 Familial FTD due to mutations in GRN

2.5.1 Loss of Function

Researchers have utilized the familial variant of FTD to explore the unique challenges posed through hereditary influences on the disease. One of the most common mutations associated with familial FTD are mutations in the GRN gene (Greenway et al., 2006, Nat. Genet.). This gene modulates protective features within the immune system which prevent excessive cell death (Babykumari et al., 2007, Brain). A dysregulation in the GRN gene is therefore thought to compromise the homeostasis in the immune system, leading to loss of function through poor maintenance in current neurons as well as insufficient care for developing synapses. Progranulin is found on the membranes of purkinje cells and pyramidal cells within the central nervous system (Lui et al., 2016, Cell) and has protective functions within the immune system in terms of regulating cytokine release, promoting cell division and regeneration (Babykumari et al., 2017, Brain). In the peripheral nervous system, progranulin is expressed in skin, the reproductive system, some motor neurons and bone marrow, though at a distinctly lower abundance than the central nervous system (Baker et al., 2006, Nature).

Therefore, progranulin is thought to serve a housekeeping role by inhibiting deleterious activity in the immune system to preserve cells (Toh et al., 2011, J Mol Neurosci). This protective feature can become detrimental when

there is a mutation within the granulin gene that impacts its function. As the protective functions of progranulin deviate, glial activity attempts to maintain the flawed homeostasis, ultimately promoting more synapse loss (Wang et al., 2021).

2.5.2 Models of FTD GRN

Transgenic progranulin knockout mice ($Grn^{-/-}$) are frequently used to model FTD and its related behavioral symptoms (Lui et al., 2016, Cell). $Grn^{-/-}$ mice show symptoms such as depression, aggression, anxiety, poor motor coordination and abnormalities in social interactions, similar to the symptoms observed in FTD patients (Kayasuga et al., 2007, Behav Brain Res). The mice further show impaired learning at the advanced age which appropriately parallels those of human patients (Lee et al., 2013, Human Molecular Genetics). The brain tissue depicts an accumulation of TDP-43 and enhanced activation of microglia (Sun and Chakrabarty 2017, Biochemistry). Lobar atrophy is reflected through impaired synaptic connectivity and plasticity (Petkau el al., 2010, Journal of Comparative Neurology).

The timeline of mouse pathology is clear through immunohistochemistry (IHC) staining and behavioral analysis. Obsessive compulsive behaviors such as excessive grooming emerge at nine months and immunostainings show activation of the classical complement pathway through C1qa (Lui et al., Cell, 2016). At the twelve months mark, brain tissue shows an abundance of C1qa and C3 mRNA levels and at the late age of nineteen months, there is major synapse loss and glial activation (Lui et al., Cell, 2016). There is significant

synaptophysin decrease at 19 months old in these knockout mice and increase in activated Iba-1 positive microglia (Lui et al., Cell, 2016).

2.5.3 Biomarkers for FTD GRN

The sudden and destructive nature of cognitive decline makes the need for reliable and early screening tests even more necessary. Proactive and sensitive testing is vital for physicians to be able to narrow down the patients' needs to design treatment and care for their precise needs. Positron emission tomography (PET) is a non-invasive method to image protein targets in the brain using high affinity radiolabeled molecules. An increasing number of 11[C] and 18[F] labelled so called radiotracers have enabled the quantitative assessment of protein concentration and function in the human brain of wide range of proteins, including membrane transporters and receptors, ion channels, cellular enzymes and misfolded proteins (Gunn et al., 2015, Phys Med Biol). Relevant PET imaging tracers within FTD include those targeted at protein aggregations of tau and TDP-43 (Zetterberg et al., 2019, Neuropath and Applied Neurobio).

While no ligands for TDP-43 have been generated thus far, several PET tracers are available to image tau neurofibrillary tangles, including [18F]THK523 (Villemagne et al., 2014, Eur J Nucle Med Mol Imaging; [18F]THK5117 (Brendel et al., 2018, Front Aging Neurosci, [11C]PBB3 (Hirano et al., 2013, Jounral of Neurol Sci) and [18F]T807 (Chien et al., 2013, Journal of Alzheimer's Disease). More recently developed PET imaging agents are those targeting the synaptic

vesicle glycoprotein 2A (SV2A), which is a synaptic vesicle membrane protein involved in the regulation of neurotransmitter release in neurons (Chen et al., 2018, JAMA Neurol). Quantification of SV2A is proposed to allow for quantitative measurements of synaptic densities in the brain, which in return is a direct measure of synaptic function. Several SV2A PET tracers have been developed and validated over the last decade (Toyonaga et al., 2022, Frontiers Neuroscience), and a most recent study utilizing [11C]UCB-J PET concludes that there exists a significant correlation between synaptic density measurements and cognitive performance in Alzheimer's disease patients, including those at early stages at the disease.

This supports the hypothesis that synapse loss is an early marker of cognitive impairment before neuronal degeneration occurs. Another surrogate measure of synaptic activity is via the use of fluorine-18 fluorodeoxy-glucose (18[F]-FDG) PET. 18[F]-FDG PET enables measurements of glucose metabolism rates and provides an indirect measurement of synaptic density. Synaptic transmission, which includes neurotransmitter synthesis, release and recycling, heavily depends on ATP, which is why a disruption in glucose metabolism is hypothesized to be a direct measure of synaptic dysfunction (Landau et al., 2011, Neurobiol Aging). 18[F]-FDG PET can assess glucose uptake abnormalities including regions at risk of cell death (Stokes, Hart and Quarles, 2016, Tomography).

CHAPTER 3

HYPOTHESIS

My **hypothesis** is that immunostaining of synaptic markers will validate the results of synaptic dysfunction determined via 18[F]-FDG PET Imaging. Further, I hypothesize that synaptic dysfunction occurs before cell death is detected and/or behavioral symptoms manifest in the $Grn^{-/-}$ mouse model of FTD. To test these hypotheses, I proposed the following two aims.

Specific Aim 1: Visualization of glucose metabolism as a surrogate for synaptic function in $Grn^{-/-}$ transgenic mice using 18[F]-FDG PET ligand. *(This aim was accomplished by our collaborators Drs. Chad Quarles and Matthew Scarpelli, BNI Neuroimaging Innovation Center).*

Specific Aim 2: Validation of PET imaging data using immunohistochemical analyses for synaptic dysfunction in $Grn^{-/-}$ mice.

CHAPTER 4

METHODS

4.1 Breeding

Mice were obtained from Jackson laboratories and used for breeding using standard protocols for homozygote x homozygote making. There were twelve C57BL/6 $Grn^{-/-}$ mice (six male, six female) from stock #013175. Meanwhile, twelve wildtype mice (six male, six female) from stock #000664) of the same amount. Both groups were of the same background and age. They were housed in groups of three in a 12 hour light cycle with food ad libitum. All animal work was approved by the Dignity Health dba St. Joseph's Hospital and Medical Center Institutional Animal Care and Use Committee.

4.2 PET Imaging

4.2.1 Acquisition

Recent literature has suggested that abnormal molecular activity emerges around the age of 9 months and abnormal behaviors become apparent around 12 months (Lui et al., 2016, Cell; Yin et al., 2010, JEM; Ahmed et al., 2010, Neurobio). By performing imaging at the 11 month timepoint instead of 12 months, the data can help narrow the window of activity. These time points are beneficial for assessing and comparing preclinical activity with potential mild cognitive impairment.

PET scanning was performed using a Bruker Albira Si 3 ring preclinical PET scanner. Approximately 8 MBq of 18[F]-FDG was injected intraperitoneally

in each mouse. PET scanning was started 70 minutes after 18[F]-FDG injection and a single 10-minute PET frame was acquired (i.e., 70-80 minutes post-injection). Mice were fasted for 22-25 hours prior to 18F FDG injection to ensure minimal blood glucose. For all PET scans the brain was positioned at the center of the field of view. An ordered subset expectation maximization algorithm was used for PET image reconstruction. Reconstructed PET images included corrections for scatter, deadtime, and decay of tracer. During scanning the mice were kept sedated using airflow of 1- 1.5 mL/s with 1-3% isoflurane and respiration was monitored to ensure adequate levels of anesthesia. During scanning mice were maintained at 37 C through the blowing of warm air (internal mechanism of the Albira SI PET scanner). MRI was performed with a 7-Tesla Bruker BioSpec preclinical MRI scanner. MRI scanning was performed immediately following completion of the PET scan. Animals were kept sedated when transferred between PET and MRI scanners and remained positioned on the same Bruker multimodality rat bed. The MRI scanning included anatomic T2-weighted (T2W) scans.

4.2.2 Analysis

Reconstructed PET images were normalized by the injected 18[F]-FDG dose and mouse weight to give standardized uptake values (SUVs) for each image voxel. Regions of interest were manually drawn in the frontal cortex. The median SUV for each region of interest was extracted and used as a summary metric for each mouse (SUV median). To summarize PET metrics across groups

of mice, the median SUV median was calculated. Significant differences in PET uptake across groups were assessed using Wilcoxon rank sum tests.

4.3 Perfusion

After the last PET analyses, 3 male and 3 female mice from each experimental group (WT and $Grn^{-/-}$) were sacrificed, brains were dissected and divided into two halves: one was used for Golgi analyses (not included in this thesis project) and the other halves were immediately flash frozen on dry ice and transferred to a -80C freezer for storage. The remaining mice (3 male/3 female, WT and $Grn^{-/-}$) were perfused with 4% PFA and left to settle overnight in a 4C fridge. The next day, the PFA was replaced with sucrose for cryoprotection. 25um sections were cut on a Leica CM3050 S cryostat, mounted on slides and stored in the -80C freezer.

4.4 Immunohistochemistry

The sectioned brain tissues were processed for immunohistochemistry as described below. Frontal cortices were stained for synaptic vesicle protein2 (SV2), postsynaptic density protein (PSD95) and microtubule associated protein 2 (Map2). Sections were first blocked-in blocking solutions (5% Donkey Serum, 1% Triton, 1% BSA in PBS) for one hour. This was followed by the incubation of primary antibodies diluted into blocking solution: Rabbit PSD95 (1:500; Thermofisher #51-6900), Mouse SV2 (1:50; DSHB AB_2315387) and Map2 (1:100, Synaptic Systems #188 004). The primary

antibodies were incubated overnight in a 4*C fridge. The following day, primary antibodies were washed off, followed by three rounds of seven minutes washing steps with blocking solution. Then, secondary antibodies were applied: Alexa Fluor 488 Donkey Anti-Rabbit IgG, Alexa Fluor Cy3 Donkey Anti-Mouse IgG and Alexa Fluor 647 Donkey Anti-GP IgG. All secondary antibodies had a dilution of 1:500 and were incubated for 45 minutes each, one after the other. After the secondary antibody treatment, sections were washed 3x for seven minutes with a blocking solution. DAPI was applied for three sets of seven minutes at a ratio of 1:12000. The slides were then mounted with cover slips and stored in the dark overnight.

For the next immunostaining procedure, the frontal cortices were stained for SV2, Allograft inflammatory factor 1 (Iba-1) and Cluster of Differentiation 68 (CD68). Sections were first blocked-in blocking solutions (5% Donkey Serum, 1% Triton, 1% BSA in PBS) for one hour.

The Rabbit Iba-1 (1:500; Wako # 019-19741) and Mouse SV2 (1:50; DSHB AB_2315387) primaries were diluted and incubated overnight. The following day, primary antibodies were washed off, followed by three seven minutes washing steps with blocking solution. Then, secondary antibodies were applied: Alexa Fluor 488 Donkey Anti-Rabbit IgG (1:500) and Alexa Fluor Cy3 Donkey Anti-Mouse (1:500) and they incubated in succession for 45 minutes each. After the secondary antibody treatment, sections were washed 3x for seven minutes with a blocking solution.

Due to secondaries including both rat and mice, the procedure continued with adding Rat CD68 (1:250; Bio-Rad Lab #MCA1957) primary diluted and incubated overnight. The following day, the primary antibody was washed off, followed by three seven minutes washing steps with a blocking solution. The secondary antibody, Alexa Fluor 647 Donkey Anti-Rat IgG (1:200), was applied and incubated for 45 minutes. After the secondary antibody treatment, sections were washed 3x for seven minutes with a blocking solution. DAPI was applied for seven minutes at a ratio of 1:12000. The slides were then mounted with cover slips and stored in the dark overnight.

4.4.1 Imaging of Immunohistochemistry

An LSM 800 Zeiss confocal microscope with a 63X oil objective was used with step size 1um. When imaging the hippocampus and frontal cortex, five images were taken in three different brain sections, yielding fifteen images per brain with 180 images. In the ventroposterolateral thalamus (VPL), three images were taken in three sections of each brain, yielding nine images from each brain and a total of 108 images. Proteins were quantified using Imaris software.

4.4.2 Statistical Analysis

The abundance of synaptic markers through mean intensity of fluorescence observed from imaging was quantified using ANOVA. Abundance

of the glial activity marker was quantified by its colocalization to the microglia membrane marker and the area dimensions relative to the image. These results were then quantified using ANOVA.

CHAPTER 5

RESULTS

5.1 18[F]-FDG PET analysis does not reveal changes in synaptic activity

To explore how progranulin deficiency influences synaptic activity before behavioral symptoms occur, $Grn^{-/-}$ and WT mice were monitored for fluorine-18 fluorodeoxy-glucose (18[F]- FDG) PET using PET imaging analyses at two time points: 9 and 11 months (Figure 1 A+B).

To facilitate brain region-specific analyses of the PET tracer images, the animals underwent a magnetic resonance imaging (MRI) scan shortly after the PET scan. Quantitative analyses of the 18[F]-FDG PET tracer was then performed in the frontal cortex region of each subject. Analysis was performed through Wilcoxon rank sum tests that quantified PET uptake through a standardized uptake value (SUV) median. Upon assessing the data, analysis did detect some variation among groups within individual timepoints. The nine months' time point shown in Figure 1C, male $Grn^{-/-}$ mice showed a significantly reduced SUV compared to male WT mice ($p=0.004$). A similar trend was observed at the 11 months timepoint, albeit without reaching significance (Figure 1D). At both timepoints female controls had significantly lower PET uptake than male controls (Figure 1C: tp1 $p=0.002$, Figure 1D: tp2 $p=0.03$). Figure 1E details the median percent change in SUV between timepoints. Overall, no significant changes in 18[F]-FDG PET signals were observed between WT and $Grn^{-/-}$ mice, suggesting that no aberrant glucose metabolism, and therefore synaptic activity,

is present in progranulin knockout mice at these early symptomatic stages

(Petkau et al., 2012, Neurobiology of disease).

NOTE: *This work was performed by our collaborators Drs. Chad Quarles and Matthew Scarpelli, Barrow Neurological Institute, Neuroimaging Center.*

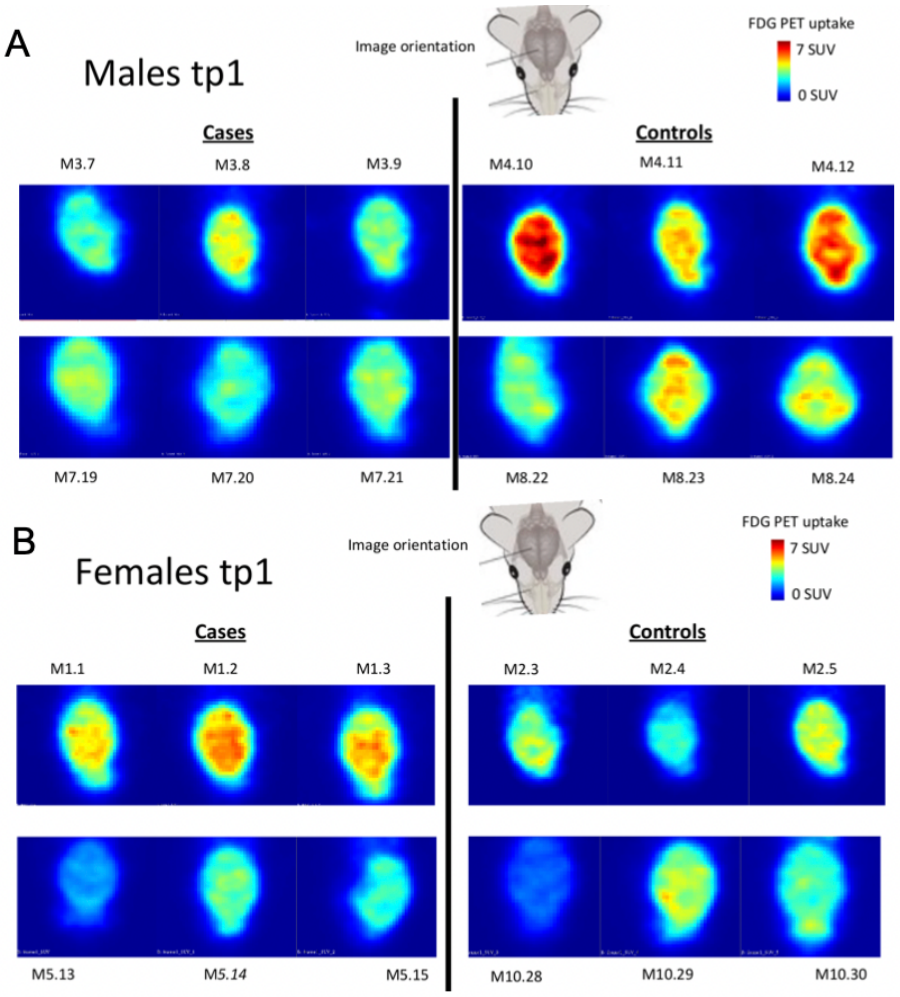

C **Median PET uptake tp 1 (interquartile range)**

	Cases	Controls	*Median*
Males	3.1[a,c] (3.0 – 3.4)	4.3[a,d] (4.1 – 4.9)	3.8 (3.2 – 4.3)
Females	3.6[b,c] (2.6 – 4.6)	3.2[b,d] (2.7 - 3.7)	3.2 (2.6 – 4.0)
Median	3.1 (2.8 – 4.1)	3.8 (3.3 – 4.3)	3.5 (2.8 - 4.3)

a, P = 0.004
b, P = 0.59
c, P = 1
d, P = 0.02

D **Median PET uptake tp 2 (interquartile range)**

	Cases	Controls	*Median*
Males	3.2[a,c] (2.8 – 3.7)	4.4[a,d] (4.0 – 4.8)	3.9 (2.8 – 4.4)
Females	3.6[b,c] (3.3 – 3.8)	3.3[b,d] (2.6 – 3.6)	3.5 (3.0 – 3.8)
Median	3.5 (2.8 - 3.8)	3.8 (3.0 – 4.2)	3.5 (2.8 – 4.0)

a, P = 0.09
b, P = 0.39
c, P = 0.59
d, P = 0.03

E **Median percent change in PET uptake from tp 1 to tp 2**

	Cases	Controls	**Median**
Males	2% (-7% to 16%)	-6% (-8% to -3%)	-4% (-9% to 5%)
Females	-1% (-13% to 15%)	19% (-12% to 31%)	6% (-17% to 28%)
Median	2% (-11% to 20%)	-4% (-11% - 18%)	0% (-11% to 21%)

Figure 1: 18[F]-FDG PET of Grn$^{-/-}$ Mice
PET scans of Grn$^{-/-}$ (cases) and wild-type males at the nine months' time point with their numerical identification. (A) PET scans of Grn$^{-/-}$ (cases) and wild-type males at the nine months' time point with their numerical identification. (B) PET scans of Grn$^{-/-}$ (cases) and wild-type females at the nine months' time point with their numerical identification. (C) Median PET uptake in the frontal cortex at nine months. The red box indicates significant differences in FDG-PET ligand uptake among male Grn$^{-/-}$ and WT mice (p=0.004). The green box indicates significant differences in FDG-PET ligand uptake between male and female controls (p=0.02). (D) Median FDG-PET uptake in the frontal cortex at eleven months. The blue indicates significant differences between male and female controls (p=0.03). (E) The median percent change in the FDG-PET uptake in the frontal cortex between the 9 and 11 months timepoints. ^{18}[F]-FDG PET imaging of Grn$^{-/-}$ mice do not show significant differences compared to WT mice.

5.2 Frontal Cortex of 11 months old Grn$^{-/-}$ mice does not reveal significant changes in synaptic marker proteins

The frontal cortex is one of the main regions implicated in FTD. Postmortem tissue of patients with FTD indicate atrophy and degeneration within the frontal lobe (Yu et al., 2010, Archives of Neurol). Major diagnostic factors of FTD include emotional regulation, decision making and social

behaviors (Henstridge et al., 2017, Acta Neuropathol); all these functions are associated with the frontal cortex to some extent.

To further assess synaptic density within $Grn^{-/-}$ mice, immunohistochemistry for pre and post synaptic proteins was performed. Frontal cortices of 6 $Grn^{-/-}$ and 6 WT mice (3 male/3 female for each experimental group) were fluorescently immunostained for postsynaptic density protein 95 (PSD95) and presynaptic vesicle protein (SV2). Confocal image analyses revealed typical puncta protein expression of both proteins (Figures 2A-H). Quantitative analyses of the immunostaining revealed no significant differences in the overall intensity of PSD95 and SV2 in $Grn^{-/-}$ compared to WT mice (Figures 2I+J; ANOVA, PSD95: p=0.92, SV2: p=0.27), nor sex (ANOVA, PSD95: p=0.84, SV2: p=0.57). Unlike the PET analyses, the immunostaining did not reveal any differences between male $Grn^{-/-}$ and WT mice (p=0.22).

5.3 Hippocampus of 11 months old $Grn^{-/-}$ mice does not reveal significant changes in synaptic marker proteins

The hippocampus is vital to executive function through memory development and retention (Kaneko et al., 2002, Eur J Nuc Med Mol Imaging). Progranulin has been implicated in the neurogenesis of the CA1 pyramidal neurons of the hippocampus (Rei et al., 2011, Neuroreport). $Grn^{-/-}$ mice exhibited cell death in the hippocampal regions, which prompted us to examine this brain region for potential synaptic activity changes as well (Stephan et al., 2013, J. Neurosci) (Lui et al., 2016, Cell).

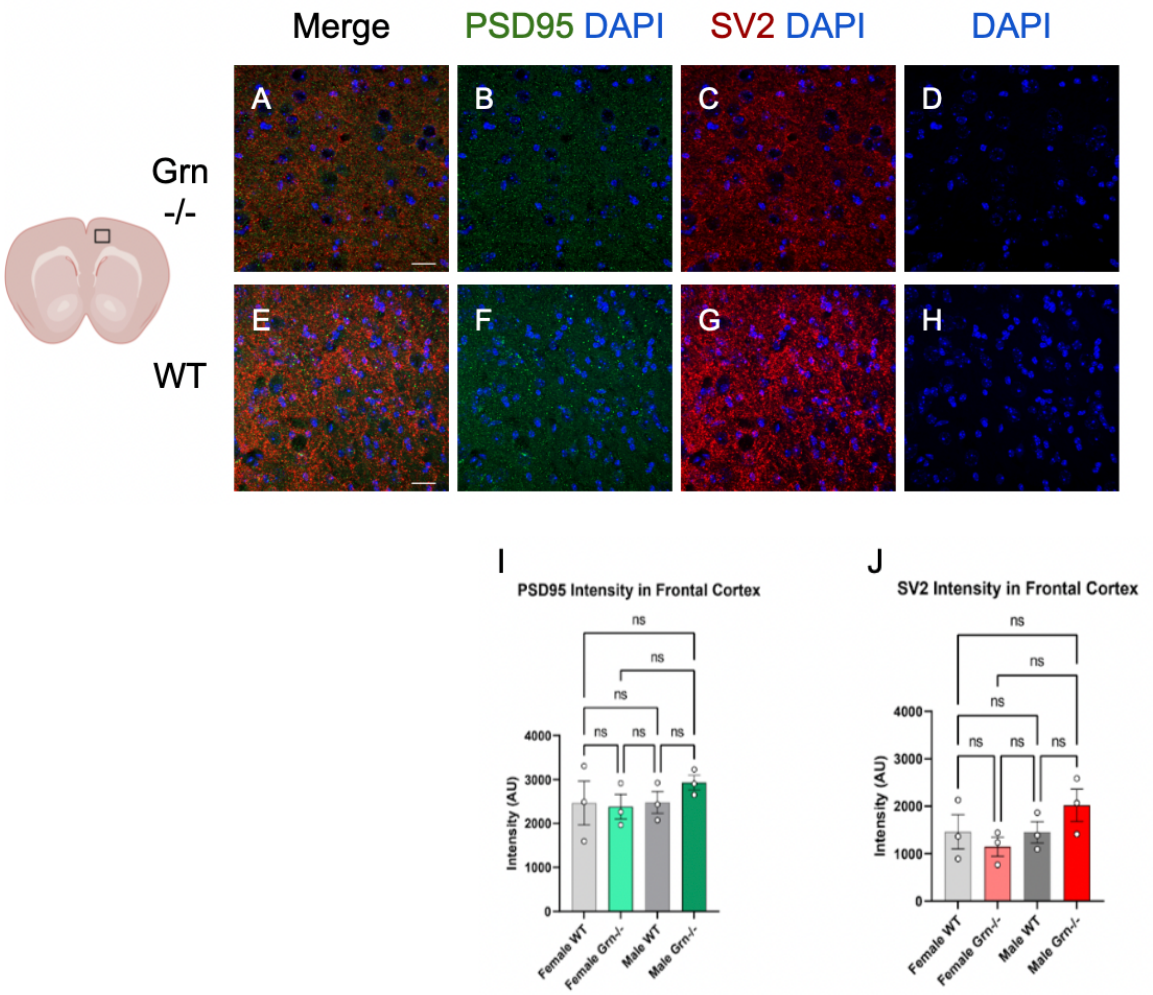

Figure 2: Frontal Cortex of 11 Months Old Grn$^{-/-}$ Mice Does Not Reveal Significant Changes in Synaptic Marker Proteins

Confocal images of PSD95, SV2 and DAPI in coronal sections in the frontal cortex of 11-month old Grn$^{-/-}$ (A-D) and WT (E-H) mice. (I) Quantification of fluorescent intensity of PSD95 in male and female WT and Grn$^{-/-}$ mice (n=3 for each experimental group). Statistical analysis was done using ANOVA: Female WT vs. female Grn$^{-/-}$ (p=0.99). Female WT vs. male WT (p=0.99). Female WT vs. Male Grn$^{-/-}$ (p=0.75). Female Grn$^{-/-}$ vs. male Grn $^{-/-}$ (p=0.64). Male WT vs. Male Grn$^{-/-}$ (p=0.76). (J) Quantification of fluorescent intensity of SV2 in male and female WT and Grn-/- mice (n=3 for each experimental group). Statistical analysis was done using ANOVA: Female WT vs. female Grn$^{-/-}$ (p=0.87). Female WT vs. male WT (p=0.99). Female WT vs. Male Grn$^{-/-}$ (p=0.55). Female Grn$^{-/-}$ vs. Male Grn$^{-/-}$ (p=0.87). Female Grn$^{-/-}$ vs. male Grn $^{-/-}$ (p=0.22). Male WT vs. Male Grn$^{-/-}$ (p=0.53).

Therefore, similar to the frontal cortex, immunohistochemistry for pre and post synaptic proteins was performed in the hippocampal CA1 region.

Hippocampi of 6 Grn$^{-/-}$ and 6 WT mice (3 male/3 female for each experimental

group) were fluorescently immunostained for postsynaptic density protein 95 (PSD95) and presynaptic protein SV2. Confocal image analyses revealed typical puncta protein expression of both proteins and brain regions (Figures 3A-H).

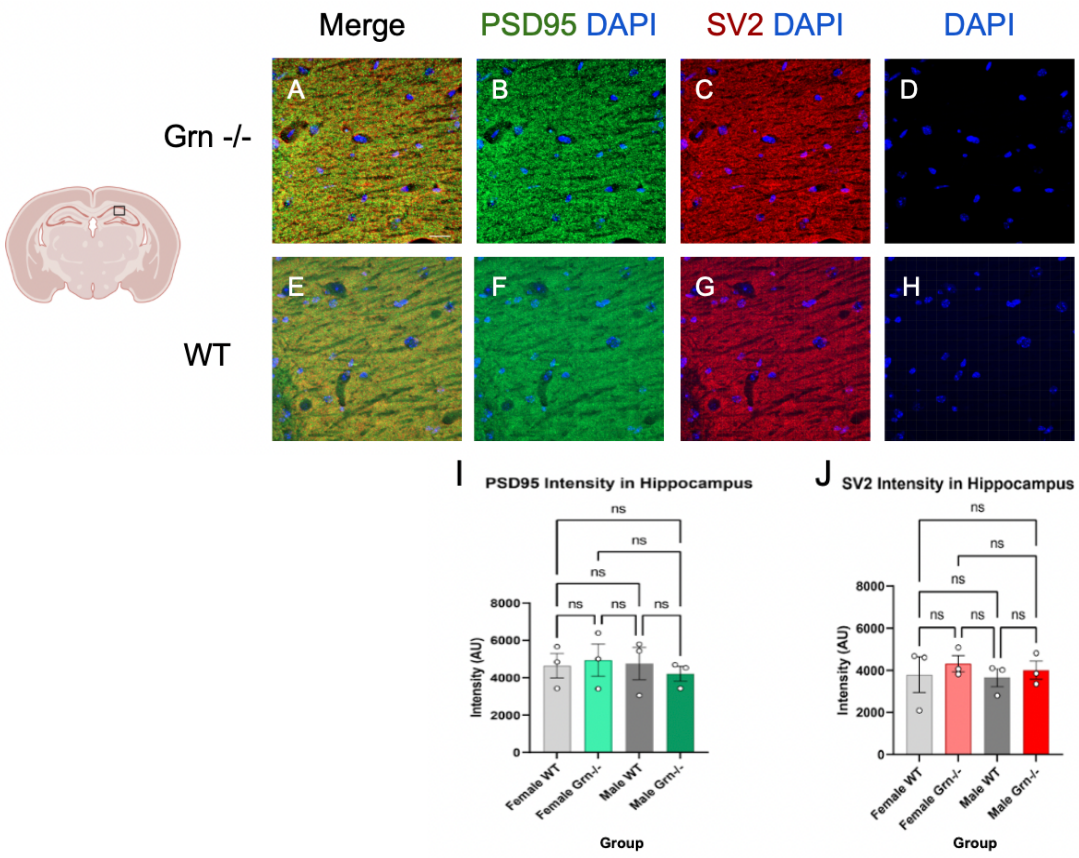

Figure 3: Hippocampus of 11 Months Old Grn$^{-/-}$ Mice Does Not Reveal Significant Changes in Synaptic Marker Proteins

Confocal images of PSD95, SV2 and DAPI in coronal sections in the CA1 region of the hippocampus of 11-month old Grn$^{-/-}$ (A-D) and WT (E-H). (I) Quantification of fluorescent intensity of PSD95 in female WT (n=3), female Grn$^{-/-}$ (n=3), male WT (n=3) and male Grn$^{-/-}$ (n=3). (I) Quantification of fluorescent intensity of PSD95 in male and female WT and Grn$^{-/-}$ mice (n=3 for each experimental group). Statistical analyses were done using ANOVA: Female WT vs. female Grn$^{-/-}$ (p=0.86). Female WT vs. male WT (p=0.99). Female WT vs. Male Grn$^{-/-}$ (p=0.55). Female Grn$^{-/-}$ vs. Male Grn$^{-/-}$ (p=0.88). Female Grn$^{-/-}$ vs. male Grn $^{-/-}$ (p=0.22). Male WT vs. Male Grn$^{-/-}$ (p=0.53). (J) Quantification of fluorescent intensity of SV2 in male and female WT and Grn$^{-/-}$ mice (n=3 for each experimental group). Statistical analyses were done using ANOVA: Female WT vs. female Grn$^{-/-}$ (p=0.91). Female WT vs. male WT (p=0.99). Female WT vs. Male Grn$^{-/-}$ (p=0.99). Female Grn$^{-/-}$ vs. Male Grn$^{-/-}$ (p=0.82). Female Grn$^{-/-}$ vs. male Grn $^{-/-}$ (p=0.98). Male WT vs. Male Grn$^{-/-}$ (p=0.97). Female vs. Male (p=0.69).

Quantitative analyses of intensities of PSD95 and SV2 immunostaining revealed no significant differences between $Grn^{-/-}$ and WT mice (Figures 3I+J; ANOVA PSD95: p=0.91 and SV2: p=0.15), nor between male and female mice (Figures 3I+J; ANOVA PSD95: p=0.95 and SV2: p=0.69). While no PET scans were quantified from this brain region, the fluorescent image analyses of the CA1 hippocampal region suggest that at 11 months, $Grn^{-/-}$ mice to do exhibit detectable changes in pre-or postsynaptic marker protein expression.

5.4 Thalamus of 11 months old $Grn^{-/-}$ mice does not reveal significant changes in synaptic marker proteins

The thalamus functions in part as the information distribution hub within the brain (Rose et al., 2006, Neuroimage). Degeneration of this major circuitry station can cause a dangerous series of downstream effects (Rose et al., 2006, NeuroImage). Recent literature has suggested that $Grn^{-/-}$ microglia preferentially eliminate inhibitory synapses in ventral thalamus which is part of the neural circuitry leading to the prefrontal cortex (Lui et al., 2016, Cell). Reduced volume in the thalamus has been associated with other neurodegenerative diseases such as Alzheimer's disease in humans (Jon et al., 2008, Brain). Within mouse models, mice with $Grn^{-/-}$ exhibit hyperexcitability in the ventral thalamus and a loss of mitigation in regulation of immunological pathways and thus, modulatory capabilities over the immune system (Lui et al., 2016, Cell).

Similar to the two brain regions in Figure 4, we assessed synaptic density within this region using immunohistochemistry staining for pre and postsynaptic

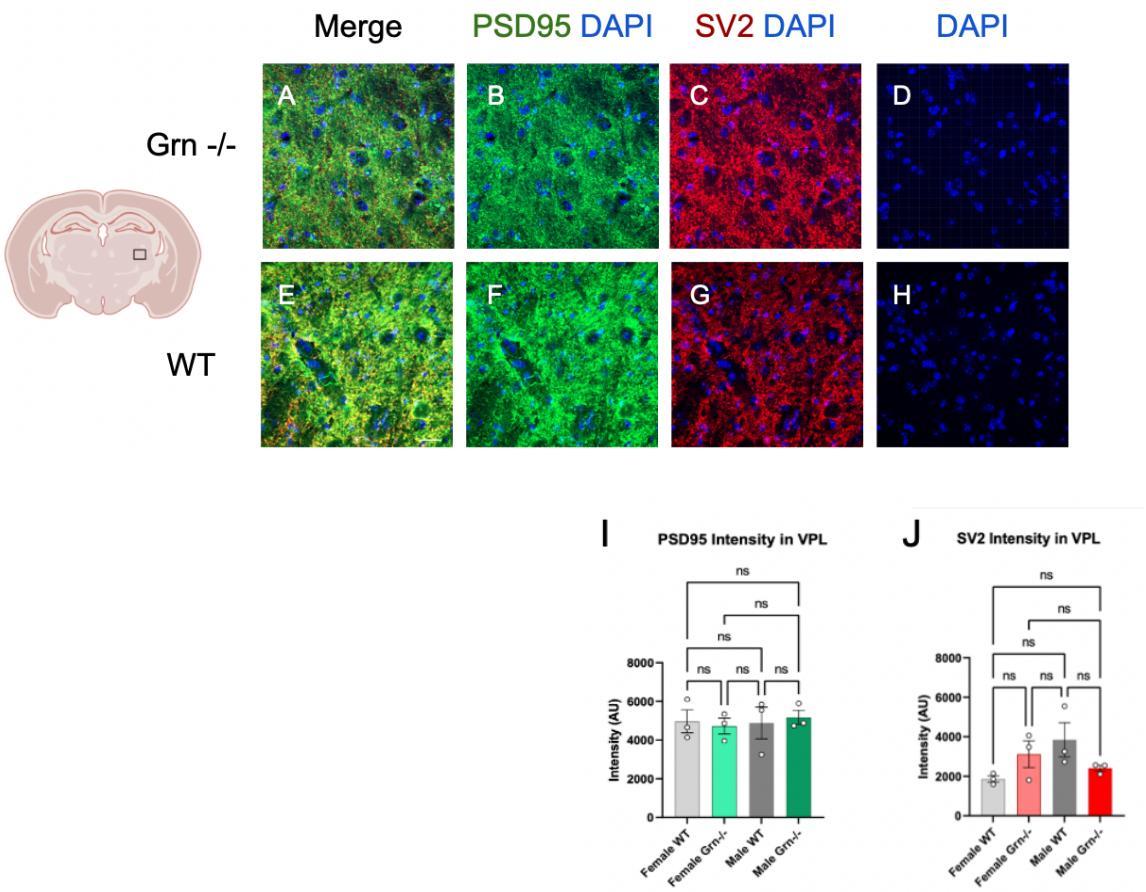

Figure 4: Ventroposterolateral Thalamus of 11 Months Old Grn$^{-/-}$ Mice Does Not Reveal Significant Changes in Synaptic Marker Proteins

Confocal images of PSD95, SV2 and DAPI in coronal sections in the ventroposterolateral thalamus (VPL) of 11-month-old Grn$^{-/-}$ (Figures 4A-D) and WT (Figures 4E-H). (I) Quantification of fluorescent intensity of PSD95 in male and female WT and Grn$^{-/-}$ mice (n=3 for each experimental group). Statistical analyses were done using ANOVA: Female WT vs. female Grn$^{-/-}$ (p=0.99). Female WT vs. male WT (p=0.99). Female WT vs. Male Grn$^{-/-}$ (p=0.99). Female Grn$^{-/-}$ vs. Male Grn$^{-/-}$ (p=0.99). Female Grn$^{-/-}$ vs. male Grn $^{-/-}$ (p=0.94). Male WT vs. Male Grn$^{-/-}$ (p=0.98). Female Grn$^{-/-}$ vs. male Grn $^{-/-}$ (p=0.98). Male WT vs. Male Grn$^{-/-}$ (p=0.97). (J) Quantification of fluorescent intensity of SV2 in male and female WT and Grn$^{-/-}$ mice (n=3 for each experimental group). Statistical analyses were done using ANOVA: Female WT vs. female Grn$^{-/-}$ (p=0.46). Female WT vs. male WT (p=0.13). Female WT vs. Male Grn$^{-/-}$ (p=0.89). Female Grn$^{-/-}$ vs. Male Grn$^{-/-}$ (p=0.80). Female Grn$^{-/-}$ vs. male Grn $^{-/-}$ (p=0.81). Male WT vs. Male Grn$^{-/-}$ (p=0.33).

proteins SV2 and PSD95, respectively. The puncta expression pattern of both proteins remained unchanged (Figures 4A-H) and quantitative analyses revealed no significant difference between Grn$^{-/-}$ and WT mice (Figure 4I+J; ANOVA; PSD95: p=0.92, SV2: p=0.39). Females and males were not significantly

different either (PSD95: p=0.99, SV2: p=0.43). This data supports similar data to the other brain regions that were analyzed, pre-symptomatic 11 months old $Grn^{-/-}$ mice do not exhibit aberrant expression of the select pre and postsynaptic marker proteins via quantitative fluorescent immunostaining.

5.5 Frontal Cortex of 11 months old $Grn^{-/-}$ mice does not reveal significant activation of microglia proteins

Because microglia function as a macrophage in the central nervous system, their increased activation may suggest that more cells are being removed (Streit, Mark and Griffin, 2004, J Neuroinflammation). Progranulin has the ability to regulate lysosomal function and production in microglia (Lui et al., 2016, Cell) and in $Grn^{-/-}$ mice, the effects of a dysregulated lysosomal mechanism were observed in the frontal cortex (Cagin et al., 2017, J Alzheimers Dis).

To examine if at the early presymptomatic age of 11 months $Grn^{-/-}$ mice will show microglial activation, we immunostained frontal cortices of 6 $Grn^{-/-}$ and 6 WT mice (3 male/3 female for each experimental group) for cluster of differentiation 68 (CD68) as a marker of microglia activation and microglia marker protein ionized calcium binding adaptor molecule 1 (Iba-1). We further included staining for SV2 to be able to examine if microglial cells were found to be activated in close proximity to synapses. Confocal image analyses revealed consistent protein expression of all three proteins (Figures 5A-J). Quantitative analyses of the immunostaining revealed no significant differences in the

overall pixel intensity of Iba-1 positive CD68 microglia or SV2 in Grn$^{-/-}$ compared to WT mice. (Figures 5I+J; ANOVA: CD68: p=0.50, SV2: p=0.16).

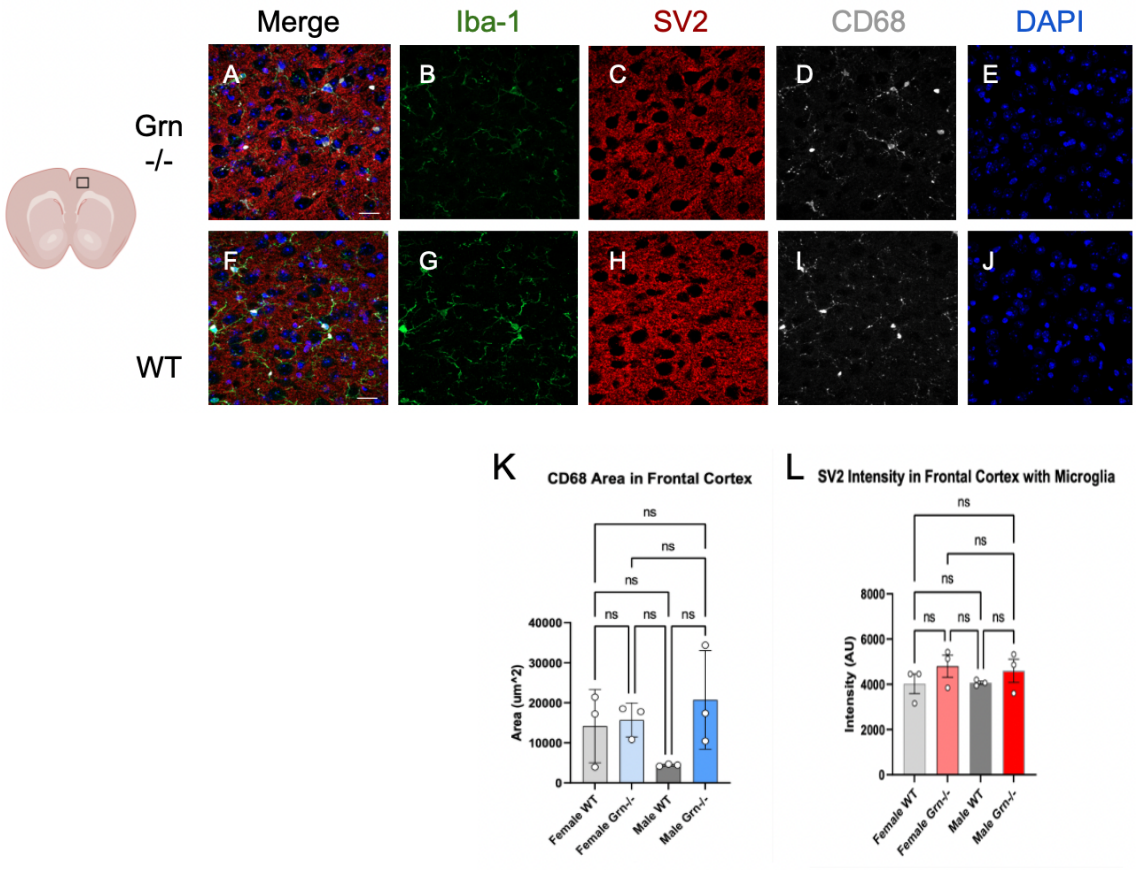

Figure 5: Frontal Cortex of 11 Months Old Grn$^{-/-}$ Mice Does Not Reveal Significant Activation of Microglia

Confocal images of Iba-1, SV2, CD68 and DAPI in coronal sections in the frontal cortex of 11- month old Grn$^{-/-}$ (A-E) and WT (F-J).

(K) Quantification of fluorescent intensity of CD68 in male and female WT and Grn$^{-/-}$ mice (n=3 for each experimental group). Statistical analyses were done using ANOVA: Female WT vs. female Grn$^{-/-}$ (p=0.99). Female WT vs. male WT (p=0.48). Female WT vs. Male Grn$^{-/-}$ (p=0.75). Female Grn$^{-/-}$ vs. Male Grn$^{-/-}$ (p=0.37). Female Grn$^{-/-}$ vs. male Grn $^{-/-}$ (p=0.86). Male WT vs. Male Grn$^{-/-}$ (p=0.13).

(L) Quantification of fluorescent intensity of SV2 in male and female WT and Grn$^{-/-}$ mice (n=3 for each experimental group). Statistical analyses were done using ANOVA: Female WT vs. Male Grn$^{-/-}$ (p=0.77). Female Grn$^{-/-}$ vs. Male Grn$^{-/-}$ (p=0.62). Female Grn$^{-/-}$ vs. male Grn $^{-/-}$ (p=0.98). Male WT vs. Male Grn$^{-/-}$ (p=0.81).

CHAPTER 6

DISCUSSION

Measuring synaptic dysfunction via PET imaging is of great value to enable early diagnosis of cognitive impairment in patients, given that synaptic density changes are proposed to correlate with the progression and severity of a variety of neurodegenerative disease characterized by dementias, including FTD. While we used a surrogate measure of synaptic activity by monitoring glucose metabolism via 18[F]-FDG radiotracers, more direct measures of synapses are now available to be used. Those include PET agents for the synaptic vesicle glycoprotein 2A (SV2A) (Toyonaga et al., 2022, Frontiers Neuroscience). The use of these tracers could indeed improve on the more accurate detection of synapse loss in the present $Grn^{-/-}$ mouse model, similar to its previous use in transgenic AD mice (APP/PS1) (Toyonaga et al., 2019, J Nucl Med). The same groups of researchers published a most recent study of the successful translation of these SV2A PET ligands into AD patients (Mecca et al., 2022, Alzheimer's and Dementia).

Other proteins known to be involved in synaptic function have also been targeted for PET imaging approaches, including proteins specific for glial activation. Examples include: [11C]PBR28, [18F]FEPPA and [18F]DPA-174 ligands to detect translocator protein 18kDa (TPSO) (Zürcher et al., 2021.Mol Psychiatry; Oh et al., 2011, Neuroimmune Pharmacol; Simpson et al., 2022, Neuropsychopharmacology; Kaneko et al., 2022, Eur J Nucl Med Mol Imaging;

Zhang 2015, J Neuroinflammation) or [11C]NCGG401 ligand to detect colony stimulating factor 1 receptors (CSF1R) (Ogata et al., 2022, Bioorg Med Chem Lett).

The chosen time points for this study were based on several previous studies using the $Grn^{-/-}$ mice. Petkau and colleagues described mild abnormalities in anxiety-related behaviors at 8 months followed by numerous analyses of synaptic transmission in 12 months old mice (Petkau et al., 2012, Neurobiology of disease). Lui and colleagues investigated the role of microglia mediated synaptic pruning in the same mouse model (Lui et al., 2016, Cell). Here, the authors noted changes in microglia activation as early as 9 months in varying brain regions, including cerebral cortex, hippocampus and thalamus. This provided the rationale for performing immunostaining on those three brain regions in the present study when investigating synaptic dysfunction in conjunction with the [18F]-FDG PET imaging analyses. Lui and colleagues also performed immunostaining for presynaptic marker protein synaptophysin and showed reduction in immunostaining intensity as early as 4 months. We do not know why SV2 immunostaining in our study did not reveal similar reduction in levels of a presynaptic protein at 11 months. Potentially, differences in antibody affinities could explain a more sensitive detection of decreased levels of proteins. It could also simply be the difference in the protein itself, although both proteins, synaptophysin and SV2 are synaptic vesicle proteins and should therefore provide overlapping information on the presence or absence of synaptic vesicles at the presynaptic terminals.

While the lack of microglia activation in our studies support and validate our findings on the lack of synaptic dysfunction as determined by [18F]-FDG PET and immunostaining of pre and postsynaptic marker proteins, these data to not match the findings by Lui and colleagues who detected significant increases in complement pathway proteins C1qa and C3, which the authors show occurs at both the RNA and protein level as early as 4 months (Lui et al., 2016, Cell). While we would have expected to see an increase in CD68 expression in Iba-1 positive microglia, we have no explanation to why our analyses overall did not show any signs of synaptic dysfunction nor microglia activation at the 11 month time point compared to those previously published data sets. RNA sequencing and western blot testing would be beneficial to discern the abundance of progranulin within the mice.

While progranulin has been discussed as an important modulator of immune system activity within the brain, other influences could possibly be compensating for its deficiency. The degree of progranulin's influence on synaptic maintenance through aging warrants greater exploration.

While unable to be explored during this project, regions such that contain pyramidal and purkinje neurons such as the amygdala and cerebellum merit further exploration. The emotional dysregulation and muscular tremors observed in patients with FTD suggest potential influence from these regions (Arrant et al., 2006, Brain and Behavior).

To further explore the aims of this project, it would be beneficial to increase the size of the cohort and to perform a thorough longitudinal PET

imaging analysis using a direct tracer for SV2A, and potentially also a PET tracer to measure microglia activation. With a larger cohort of mice, we could also analyze brain tissue in parallel to each PET scan, instead of only having one time point for the pathological analyses of the mice. There are other procedures that could have contextualized the collected data. Performing western blots would have offered more opportunity to confirm the loss of progranulin within the transgenic mice. Overall, the use of western blot analyses for any of the proteins examined via immunostaining would provide a more quantitative readout of the protein expression. Finally, western blots and immunostaining to detect proteins from the classic complement pathway such as C1qa or C3 could have discerned the mechanisms leading up to glial activation.

CHAPTER 7

CONCLUSION

These data suggest that $Grn^{-/-}$ mice at 9 and 11 months do not exhibit synaptic dysfunction in the frontal cortex when measured via 18[F]-FDG PET or immunostaining of pre- and postsynaptic marker proteins SV2 and PSD95, respectively. While no differences were observed between transgenic and WT mice, the data supports the use of 18[F]-FDG PET as a viable measure for synaptic activity in mouse models of FTD. Future longitudinal studies with larger sample sizes are encouraged to determine at which exact time point $Grn^{-/-}$ mice start exhibiting synaptic dysfunction. Furthermore, as PET scans become more accessible as a diagnostic measure for neurodegenerative diseases, we suggest that the 18[F]-FDG tracer has great potential to detect synaptic dysfunction in patients with cognitive impairments.

REFERENCES

Amador-Ortiz et al. (2007). TDP-43 immunoreactivity in hippocampal sclerosis and Alzheimer's disease. Annals of Neurology: Official Journal of the American Neurological Association and the Child Neurology Society, 61(5), 435-445.

Aparicio-Erriu et al. (2012). Molecular mechanisms in amyotrophic lateral sclerosis: the role of angiogenin, a secreted RNase. Frontiers in neuroscience, 6, 167.

Arai et al. (2006). TDP-43 is a component of ubiquitin-positive tau-negative inclusions in frontotemporal lobar degeneration and amyotrophic lateral sclerosis. Biochemical and biophysical research communications, 351(3), 602-611.

Arai et al. (2009). Phosphorylated TDP-43 in Alzheimer's disease and dementia with Lewy bodies. Acta neuropathologica, 117(2), 125-136.

Armon et al. (2003). An evidence-based medicine approach to the evaluation of the role of exogenous risk factors in sporadic amyotrophic lateral sclerosis. Neuroepidemiology, 22(4), 217-228.

Arrant et al. (2016). Progranulin haploinsufficiency causes biphasic social dominance abnormalities in the tube test. Genes, Brain and Behavior, 15(6), 588-603.

Asakura et al. (2011). Involvement of progranulin in the enhancement of hippocampal neurogenesis by voluntary exercise. Neuroreport, 22(17), 881-886.

Azam et al. (2021). Microglial turnover in ageing-related neurodegeneration: therapeutic avenue to intervene in disease progression. Cells, 10(1), 150.

Baker et al. 2006). Mutations in progranulin cause tau-negative frontotemporal dementia linked to chromosome. Nature, LETTERS, 17, 1-4.

Banks et al. (2008). TDP-43 is a culprit in human neurodegeneration, and not just an innocent bystander. Mammalian Genome, 19(5), 299-305.

Benussi et al. (2016). Loss of exosomes in progranulin-associated frontotemporal dementia. Neurobiology of aging, 40, 41-49.

Bi et al. (2011). Tau-targeted immunization impedes progression of neurofibrillary histopathology in aged P301L tau transgenic mice. PloS one, 6(12), e26860.

Birsa et al. (2020, March). Cytoplasmic functions of TDP-43 and FUS and their role in ALS. In Seminars in cell & developmental biology (Vol. 99, pp. 193-201). Academic Press.

Buratti and Baralle. (2008). Multiple roles of TDP-43 in gene expression, splicing regulation, and human disease. Front Biosci, 13(8).

Butler et al. (2021). Comorbidity trajectories associated with Alzheimer's disease: a matched case-control study in a United States claims database. Frontiers in neuroscience, 1347.

Caga et al. (2019). The impact of cognitive and behavioral symptoms on ALS patients and their caregivers. Frontiers in neurology, 10, 192.

Chen et al. (2018). Assessing synaptic density in Alzheimer disease with synaptic vesicle glycoprotein 2A positron emission tomographic imaging. JAMA neurology, 75(10), 1215-1224.

Chia et al. (2018). Novel genes associated with amyotrophic lateral sclerosis: diagnostic and clinical implications. The Lancet Neurology, 17(1), 94-102.

Chien et al. (2014). Early clinical PET imaging results with the novel PHF-tau radioligand [F18]-T808. Journal of Alzheimer's Disease, 38(1), 171-184.

Chornenkyy et al. (2019). Tau and TDP-43 proteinopathies: kindred pathologic cascades and genetic pleiotropy. Laboratory investigation, 99(7), 993-1007.

Colom-Cadena et al. (2020). The clinical promise of biomarkers of synapse damage or loss in Alzheimer's disease. Alzheimer's research & therapy, 12(1), 1-12.

Constantinescu et al. (2019). Development and in vivo preclinical imaging of fluorine-18-labeled synaptic vesicle protein 2A (SV2A) PET tracers. Molecular Imaging and Biology, 21(3), 509-518.

Cook et al. (2020). C9orf72 poly (GR) aggregation induces TDP-43 proteinopathy. Science translational medicine, 12(559), eabb3774.

Deleon and Miller. (2018). Frontotemporal dementia. Handbook of clinical neurology, 148, 409-430.

Galimberti et al. (2015). Psychiatric symptoms in frontotemporal dementia: epidemiology, phenotypes, and differential diagnosis. Biological Psychiatry, 78(10), 684-692.

Gendron et al. (2013). TARDBP mutation analysis in TDP-43 proteinopathies and deciphering the toxicity of mutant TDP-43. Journal of Alzheimer's Disease, 33(s1), S35-S45.

Goedert et al. (2000). Tau mutations in frontotemporal dementia FTDP-17 and their relevance for Alzheimer's disease. Biochimica et Biophysica Acta (BBA)-Molecular Basis of Disease, 1502(1), 110-121.

Greenway et al. (2006). ANG mutations segregate with familial and'sporadic'amyotrophic lateral sclerosis. Nature genetics, 38(4), 411-413.

Gunn et al. (2015). Quantitative imaging of protein targets in the human brain with PET. Physics in Medicine & Biology, 60(22), R363.

Henstridge et al. (2018). Synapse loss in the prefrontal cortex is associated with cognitive decline in amyotrophic lateral sclerosis. Acta neuropathologica, 135(2), 213-226.

Hirano et al. (2013). In vivo visualization of tau pathology in Alzheimer's disease patients by [11c] PBB3-PET. Journal of the Neurological Sciences, 333, e319.

Josephs and Nelson. (2015). Unlocking the mysteries of TDP-43. Neurology, 84(9), 870-871.

Kayasuga et al. (2007). Alteration of behavioural phenotype in mice by targeted disruption of the progranulin gene. Behavioural brain research, 185(2), 110-118.

Kertesz et al. (1999). Clinical and pathological overlap between frontotemporal dementia, primary progressive aphasia and corticobasal degeneration: the Pick complex. Dementia and geriatric cognitive disorders, 10(Suppl. 1), 46-49.

Kertesz et al. (2005). The evolution and pathology of frontotemporal dementia. Brain, 128(9), 1996-2005.

Lee et al. (2013). Targeted manipulation of the sortilin–progranulin axis rescues progranulin haploinsufficiency. Human molecular genetics, 23(6), 1467-1478.

Liu et al. (1999). Synapse density related to cerebral blood flow and symptomatology in frontal lobe degeneration and Alzheimer's disease. Dementia and geriatric cognitive disorders, 10(Suppl. 1), 64-70.

Lui et al. (2016). Progranulin deficiency promotes circuit-specific synaptic pruning by microglia via complement activation. Cell, 165(4), 921-935.

Maiti et al. (2015). Merging advanced technologies with classical methods to uncover dendritic spine dynamics: a hot spot of synaptic plasticity. Neuroscience research, 96, 1-13.

Majoor-Krakauer et al. (1994). Familial aggregation of amyotrophic lateral sclerosis, dementia, and Parkinson's disease: evidence of shared genetic susceptibility. Neurology, 44(10), 1872-1872.

Neumann and Mackenzie. (2019). Neuropathology of non-tau frontotemporal lobar degeneration. Neuropathology and applied neurobiology, 45(1), 19-40.

Neumann et al. (2006). Ubiquitinated TDP-43 in frontotemporal lobar degeneration and amyotrophic lateral sclerosis. Science, 314(5796), 130-133.

Niccoli et al. (2017). Ageing as a risk factor for ALS/FTD. Human molecular genetics, 26(R2), R105-R113.

Petkau et al. (2010). Progranulin expression in the developing and adult murine brain. Journal of Comparative Neurology, 518(19), 3931-3947.

Ransohoff and Perry. (2009). Microglial physiology: unique stimuli, specialized responses. Annual review of immunology, 27, 119-145.

Ringholz et al. (2005). Prevalence and patterns of cognitive impairment in sporadic ALS. Neurology, 65(4), 586-590.

Rivest. "Pruned to Perfection - Nature Research." Pruned to Perfection, Nature, 2018.

Rose et al. (2006). Evidence of altered prefrontal–thalamic circuitry in schizophrenia: an optimized diffusion MRI study. Neuroimage, 32(1), 16-22.

Scotter et al. (2015). TDP-43 proteinopathy and ALS: insights into disease mechanisms and therapeutic targets. Neurotherapeutics, 12(2), 352-363.

Seelaar et al. (2011). Clinical, genetic and pathological heterogeneity of frontotemporal dementia: a review. Journal of Neurology, Neurosurgery &

Psychiatry, 82(5), 476-486.

Smith et al. (2012). Strikingly different clinicopathological phenotypes determined by progranulin-mutation dosage. The American Journal of Human Genetics, 90(6), 1102-1107.

Snowden et al. (2002). Frontotemporal dementia. The British journal of psychiatry, 180(2), 140-143.

Stanford et al. (2003). Mutations in the tau gene that cause an increase in three repeat tau and frontotemporal dementia. Brain, 126(4), 814-826.

Starr and Sattler. (2018). Synaptic dysfunction and altered excitability in C9ORF72 ALS/FTD. Brain research, 1693, 98-108.

Stokes, Hart and Quarles. (2016). Hypoxia imaging with PET correlates with antitumor activity of the hypoxia-activated prodrug evofosfamide (TH-302) in rodent glioma models. Tomography, 2(3), 229-237.

Streit, W. J., Mark and Griffin. (2004). Microglia and neuroinflammation: a pathological perspective. Journal of neuroinflammation, 1(1), 1-4.

Sun and Chakrabartty. (2017). Phase to phase with TDP-43. Biochemistry, 56(6), 809-823.

Synofzik et al. (2012). Screening in ALS and FTD patients reveals 3 novel UBQLN2 mutations outside the PXX domain and a pure FTD phenotype. Neurobiology of aging, 33(12), 2949-e13.

Tantawy et al. (2012). Assessment of renal function in mice with unilateral ureteral obstruction using 99mTc-MAG3 dynamic scintigraphy. BMC nephrology, 13(1), 1-11.

Toh et al. (2011). Structure, function, and mechanism of progranulin; the brain and beyond. Journal of Molecular Neuroscience, 45(3), 538-548.

Toyonaga et al. (2022). PET imaging of synaptic density: challenges and opportunities of synaptic vesicle glycoprotein 2A PET in small animal imaging. Frontiers in Neuroscience, 16.

Villemagne et al. (2014). In vivo evaluation of a novel tau imaging tracer for Alzheimer's disease. European journal of nuclear medicine and molecular imaging, 41(5), 816-826.

Wang et al. (2021). Progranulin in neurodegenerative dementia. Journal of Neurochemistry, 158(2), 119-137.

Yu et al. (2010). The spectrum of mutations in progranulin: a collaborative study screening 545 cases of neurodegeneration. Archives of neurology, 67(2), 161-170.

Zhang. (2015). Mapping neuroinflammation in frontotemporal dementia with molecular PET imaging. Journal of neuroinflammation, 12(1), 1-7.

Zu et al. (2013). RAN proteins and RNA foci from antisense transcripts in C9ORF72 ALS and frontotemporal dementia. *Proceedings of the National Academy of Sciences*, *110*(51), E4968-E4977.